ORIGINAL ARTICLE

Association of Nicotine Addiction and Nicotine's Actions With Separate Cingulate Cortex Functional Circuits

L. Elliot Hong, MD; Hong Gu, PhD; Yihong Yang, PhD; Thomas J. Ross, PhD; Betty Jo Salmeron, MD; Brittany Buchholz, BS; Gunvant K. Thaker, MD; Elliot A. Stein, PhD

Context: Understanding the mechanisms underlying nicotine addiction to develop more effective treatment is a public health priority. Research consistently shows that nicotine transiently improves multiple cognitive functions. However, using nicotine replacement to treat nicotine addiction yields generally inconsistent results. Although this dichotomy is well known, the reasons are unclear. Imaging studies showed that nicotine challenges almost always involve the cingulate cortex, suggesting that this locus may be a key region associated with nicotine addiction and its treatment.

Objective: To identify cingulate functional circuits that are associated with the severity of nicotine addiction and study how nicotine affects them by means of region-specific resting-state functional magnetic resonance imaging.

Design: Double-blind, placebo-controlled study.

Setting: Outpatient clinics.

Participants: Nineteen healthy smokers.

Intervention: Single-dose (21- or 35-mg) nicotine patch.

Main Outcome Measures: Correlation of nicotine addiction severity and cingulate resting-state functional connectivity, and effects of short-term nicotine administration on connectivity strength.

Results: Clearly separated pathways that correlated with nicotine addiction vs nicotine's action were found. The severity of nicotine addiction was associated with the strength of dorsal anterior cingulate cortex (dACC)–striatal circuits, which were not modified by nicotine patch administration. In contrast, short-term nicotine administration enhanced cingulate-neocortical functional connectivity patterns, which may play a role in nicotine's cognition-enhancing properties.

Conclusions: Resting-state dACC-striatum functional connectivity may serve as a circuit-level biomarker for nicotine addiction, and the development of new therapeutic agents aiming to enhance the dACC-striatum functional pathways may be effective for nicotine addiction treatment.

Arch Gen Psychiatry. 2009;66(4):431-441

Author Affiliations: Maryland Psychiatric Research Center, Department of Psychiatry, University of Maryland School of Medicine (Drs Hong and Thaker and Ms Buchholz), and Neuroimaging Research Branch, National Institute on Drug Abuse, National Institutes of Health (Drs Gu, Yang, Ross, Salmeron, and Stein), Baltimore.

NICOTINE, THE ADDICTIVE component in tobacco, has been shown to transiently improve performance on a wide range of cognitive and neurophysiologic tasks in humans, including attention,[1,2] visual information processing,[3] computational abilities,[4] prepulse inhibition,[5] vigilance,[6] and working memory.[7] What remains unclear is how to explain nicotine effects on such diverse activities, which are controlled, at least in part, by different brain circuits. The seemingly pervasive behavioral effects of nicotine and the localization of nicotine receptors on neurons of different neurotransmitter systems[8,9] suggest the interesting possibility that nicotine may exert a modulatory effect on multiple functional brain circuits independent of specific task performance. New magnetic resonance (MR) imaging approaches to identify functional network connectivity[10,11] present the opportunity to test this hypothesis in human subjects.

A common thread running through the imaging literature is the association of the cingulate in nicotine's short-term effects and nicotine addiction.[9,12-15] Early autoradiographic imaging showed that the cingulate alone had increased glucose utilization after nicotine administration in rats.[12] Positron emission tomographic studies in humans identified high concentrations of nicotine binding sites in the cingulate, insula, thalamus, basal ganglia, and frontal lobe.[9] Nicotine dose-dependently

increased activity in the nucleus accumbens, amygdala, cingulate, and frontal lobes in the task-free state.[13] Nicotine improved sustained attention by increasing activation in the posterior cingulate, bilateral parietal and occipital cortex, thalamus, and caudate[3] and improved working memory by either enhancing[16] or reducing[14] activation in the cingulate and other areas. More recently, nicotine was found to improve attention by deactivating anterior and posterior cingulate and other brain regions,[2] whereas activation in the posterior cingulate predicted the behavioral effects of nicotine.[15] To summarize, of regions associated with nicotine's actions, the cingulate was the most frequently detected, suggesting that this region may be a convergent structure pivotal for the diverse central nervous system effects of nicotine. However, the exact location of nicotine's actions within the cingulate varies across studies. Perhaps more importantly, the apparent contradiction on the valence of nicotine's action on the cingulate needs to be reconciled because both significant activation and deactivation have been reported.

Recent advances in understanding the resting-state functional connectivity of the brain[10,11,17] provide a framework to test the hypothesis that specific cingulate functional circuitry may vary both as a function of nicotine dependence and as a function of short-term nicotine action, independent of any particular behavioral activation condition. Resting-state functional connectivity consists of task-independent, low-frequency synchronized activities across brain regions.[10,11] Its neural bases are under intense study. The slow coherent fluctuations in resting-state blood oxygenation level–dependent signals on functional MR images may reflect suppression of neuronal activity.[10,18-21] The stable spatial organization of resting-state functional connectivity maps suggests that it can be constrained by anatomic connectivity.[22,23] On the basis of previous knowledge of the functional and histologic subdivisions of the cingulate cortex,[24-29] we partitioned the entire human cingulate into anatomic subregions. This study was designed first to characterize the resting-state functional connectivity associated with each cingulate subregion, then to identify cingulate circuits that are associated with nicotine addiction, and finally to determine how short-term nicotine administration affects circuits that are associated with nicotine addiction.

METHODS

SUBJECTS

Nineteen (14 male and 5 female) healthy smokers (≥10 cigarettes a day) participated in the study. Subjects gave written informed consent approved by both University of Maryland and National Institute on Drug Abuse institutional review board panels. Subjects were 18 to 50 years of age, were right-handed, and were recruited through media advertisements. Major medical and neurologic conditions were exclusionary criteria. Subjects had no Axis I diagnoses other than nicotine dependence as evaluated by the Structured Clinical Interview for *DSM-IV*.[30] The severity of nicotine addiction was assessed by the Fagerström Test for Nicotine Dependence (FTND).[31] The FTND includes 6 items and produces a score from 0 to 10, with higher scores indicating more severe nicotine addiction. The FTND marks the genetic liability of nicotine addiction.[32,33] The cumulative exposure to smoking was calculated as pack-years.

DESIGN

This was a double-blind, placebo-controlled, crossover, randomized functional MR imaging study comparing the effect of nicotine vs placebo patch on resting-state functional connectivity. Subjects underwent imaging on 2 occasions approximately 1 week apart, within 5 to 14 days. They received either a nicotine patch (Nicoderm CQ, GlaxoSmithKline, Research Triangle Park, North Carolina) or an identical placebo patch on each occasion. We used a 2-dose strategy to better match the regular nicotine intakes: 21 mg for individuals who smoked 10 to 15 cigarettes a day (n=6) and 35 mg for individuals who smoked more than 15 cigarettes a day (n=13).

Subjects were instructed to maintain their normal smoking routine before patch application, and then abstain for about 4.5 hours after patch administration, including 2.5 hours before imaging, and 2 hours inside the imager. The 4.5-hour window was chosen to avoid confounders induced by withdrawal, which generally begins 6 to 12 hours after the start of abstinence.[34] In the imager, each subject underwent 1 hour of smooth-pursuit eye movement/fixation tasks (data not shown), followed by a 5-minute resting image and an 8-minute structural image. Resting image data were therefore collected about 3.5 hours after patch administration, which is within the window of steady plasma nicotine levels.[6] A self-reported symptom checklist and a self-reported mood change questionnaire[35] were administered before patch application and after imaging. Breath carbon monoxide concentration was measured immediately before patch application. Plasma nicotine levels were measured at the end of each imaging session.

MR IMAGE ACQUISITION

Data were collected on a 3-T MR imager (Magnetom Allegra; Siemens, Malvern, Pennsylvania) equipped with a quadrature volume head coil. Subjects were given a simple instruction to rest and keep their eyes open. A static neutral image (the projector's logo) was presented on the screen during the resting image. A bite bar was used to minimize head motion. Resting-state functional MR images were acquired over 39 axial, interleaving, 4-mm sections by means of a gradient-echo echo planar imaging sequence (150 volumes; echo time/repetition time, 27/2000 milliseconds; flip angle, 80°; field of view, 220×220 mm^2; image matrix, 64×64). High-resolution ($1 \times 1 \times 1$ mm^3) T1-weighted magnetization-prepared rapid gradient echo images were acquired after each resting image.

DATA PROCESSING

Data were analyzed in AFNI[36] and MATLAB (The MathWorks Inc, Natick, Massachusetts). Volumes were section-timing aligned and motion corrected to the base volume that minimally deviated from other volumes by means of an AFNI built-in algorithm.[37] After linear detrending of the time course of each voxel, volumes were spatially normalized and resampled to Talairach space at $3 \times 3 \times 3$ mm^3, spatially smoothed (full-width half-maximum, 6 mm), and temporally low-pass filtered (f_{cutoff}=0.1 Hz).[38-40] Correlation analyses were performed by calculating the cross-correlation coefficient between each voxel's time course and the template time course extracted by averaging time courses of all the voxels in the defined regions of interest ("seed ROIs"), including the 6 rigid head-motion parameter time courses and the average time course in white

matter as nuisance covariates.[41,42] The white matter mask was generated by segmenting the high-resolution anatomic images in SPM5[43] and down-gridding the obtained white matter masks to the same resolution as the functional data. These nuisance covariates regress out fluctuations unlikely to be relevant to neuronal activities.[41] Cross-correlation coefficient maps were then converted to *z*-score maps by means of an AFNI built-in function.

REGIONS OF INTEREST

Each subject's cingulate was partitioned into 7 ROIs per hemisphere: 3 subregions for anterior cingulate cortex (ACC), a middle cingulate cortex (MCC), and 3 subregions for the posterior cingulate cortex (PCC). The ROIs were manually drawn on the gray matter at the coronal and sagittal planes of each subject's T1 image volume based on previous conventions when available, supplemented by histologic, structural, and functional evidence (**Figure 1**):

1. The ACC was divided into dorsal ACC (dACC), rostral ACC (oACC), and subcallosal ACC (sACC). The dACC was separated from the oACC by drawing a coronal plane that was 1 section forward from the disappearance of the juncture of the anterior corpus callosum from both hemispheres.[28,29] The posterior end of the dACC was the first vertical section posterior to the anterior commissure, as proposed by Fornito et al.[28] This is more anterior than that defined by McCormick et al[29] but is close to the division of anterior and posterior MCC that was proposed by Vogt et al[25] and Vogt and Vogt.[26] The deepest points of the cingulate and callosal sulci defined the superior and inferior boundaries, respectively, of the dACC. When the second cingulate[28,29] was present, we traced the structure as part of the cingulate ROI following rules established by McCormick et al.[29] For the oACC, the posterior margin was the first plane anterior to the first dACC plane. The anterior margin was defined when the cingulate gyrus was no longer visible at the coronal slide.[28,29] The sACC was defined by the anterior dACC plane, moving posteriorly to the first coronal section in which the caudate head and the putamen separated. The interior and superior margins were the cingulate sulcus and the corpus callosum, respectively.[28] The mean (SD) average sizes of the dACC, oACC, and sACC were 3455 (851), 1360 (456), and 813 (212) mm^3.
2. The MCC as defined herein was the posterior MCC per Vogt et al.[25] The anterior boundary was the posterior plane of the dACC. The posterior boundary was the vertical plane on the tip of marginal ramus, which was called the posterior plane for ACC per McCormick et al.[29] Separating the MCC from the ACC as an ROI is justified by cytologic findings[25,26] and its involvement in motor control.[44] The mean (SD) size of the MCC is 2679 (717) mm^3.
3. The PCC (Brodmann areas 23 and 31) was divided into 3 ROIs[27]: (1) dorsal PCC (dPCC), which was posterior to the marginal ramus plane and anterior to the ventral branch of the splenial sulci; the latter defined the histologic division of areas d23b and v23b, or dorsal and ventral PCC; (2) ventral PCC (vPCC), whose anterior border was the dPCC and posteroinferior border was the common trunk of the calcarine and parieto-occipital sulcus,[24,27] and which wrapped around the retrosplenial cortex (RSC); and (3) the RSC, which was bordered by the common trunk posteriorly and the callosal sulcus dorsoanteriorly.[24] The anterolateral segment was buried within the callosal sulcus, while the posteroventral end was on the surface of the medial hemisphere of the isthmus of the PCC.[24] To segregate the 3 PCC ROIs, the RSC was drawn first with the use of sagittal sections, which identified the RSC within the callosal sulcus. The dPCC and vPCC were then drawn with the use of the coronal sections, where the RSC was the inferior border of the dPCC and the inferior and anterior borders of the vPCC.[24,25,27] The mean (SD) sizes of the dPCC, vPCC, and RSC were 1911 (573), 1207 (391), and 1395 (366) mm^3, respectively.

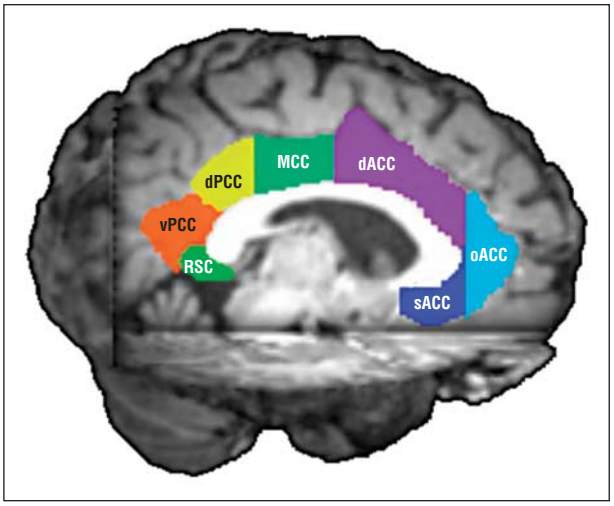

Figure 1. Midline (2 mm from midline) view of the cingulate partitions. dACC indicates dorsal anterior cingulate cortex (ACC); dPCC, dorsal posterior cingulate cortex (PCC); MCC, middle cingulate cortex; oACC, rostral ACC; RSC, retrosplenial cortex; sACC, subcallosal ACC; and vPCC, ventral PCC.

Cingulate anatomic ROIs for each hemisphere were drawn separately. The structural image of the first session was used to draw the ROIs. Structural images of the 2 sessions were aligned and the ROIs were then applied to the structural image of the second session.

CINGULATE FUNCTIONAL CONNECTIVITY MAP

One-sample, 2-tailed *t* tests were performed on each individual's *z*-score maps to obtain thresholded group functional connectivity maps at $P_{corrected} < .05$ based on Monte Carlo simulations.[45] The corrected threshold corresponds to $P_{uncorrected} < .001$[46] with a minimum cluster size of 810 mm^3 in both the nicotine and placebo conditions. For each seed ROI, thresholded group functional connectivity maps from both nicotine and placebo conditions were combined by means of an "OR" operation to generate a mask, which was used to constrain the subsequent analyses.

NICOTINE ADDICTION SEVERITY × DRUG INTERACTION ON CINGULATE CONNECTIVITY

We first investigated interactions between addiction severity (as measured by the FTND) and nicotine effect on functional connectivity by using the regression model: $V'i(diff) = \beta'0 + \beta'X + \varepsilon'$, where V' was the *z* score of the arithmetic difference between nicotine and placebo condition on the *i*th voxel and X was the centered FTND score, plus a random error term ε'. The *t* statistics of β' tested the effect of FTND on nicotine vs placebo differences, ie, drug × FTND interaction. Statistical significance of the *t* statistic for this and the subsequent analyses was thresholded after correction for multiple comparisons using Monte Carlo simulations to obtain $P_{corrected} < .05$, corresponding to $P_{uncorrected} < .001$ with a minimum cluster size of 243 to 405 mm^3. The different cluster size thresholds reflect different numbers of comparisons to be corrected for connectivity maps of different seed ROIs.

Table 1. Nicotine- vs Placebo-Related Measurements[a]

	Mean (SD)				
	Placebo Patch Condition (n = 19)	Nicotine Patch Condition (n = 19)	*t* Value[b]	*df*	*P* Value
Carbon monoxide level before patch application, ppm	27.2 (13.0)	25.0 (11.5)	1.34	18	.20
Nicotine level at end of scan, ng/mL	3.0 (4.7)	34.3 (13.1)	9.32	14[c]	<.001[d]
Change[e] in pulse rate, beats/min	−4.9 (8.5)	−2.9 (11.3)	0.78	18	.44
Change in systolic blood pressure, mm Hg	3.9 (13.4)	9.6 (12.3)	2.12	18	.05[e]
Change in diastolic blood pressure, mm Hg	5.8 (6.3)	6.4 (10.3)	0.27	18	.79
Change in withdrawal/side effect symptoms	0.7 (1.4)	0.8 (1.3)	0.00	17	>.99
Change in self-reported mood	0.8 (2.9)	1.5 (4.8)	0.90	18	.38

SI conversion factor: To convert nicotine to micromoles per liter, multiply by 0.006164.

[a] There was no significant bias on smoking level before each condition on the basis of similar carbon monoxide levels before placebo vs nicotine patch applications. Postscan nicotine levels confirmed robust differences in drug levels during placebo vs nicotine scanning.

[b] Paired *t* test.

[c] Nicotine levels were available in 15 subjects for both nicotine and placebo patch conditions. Nicotine levels were not available in 1 subject in the placebo condition, 2 subjects in the nicotine condition, and 1 subject in both the placebo and nicotine conditions because of laboratory errors (blood sample hemolysis or equipment problem).

[d] Statistically significant.

[e] Changes from prepatch application to immediately before patch removal, about a 4.5-hour interval.

MAIN EFFECT OF NICOTINE ADDICTION SEVERITY ON CINGULATE CONNECTIVITY

In the event of no significant interaction, we applied a second regression model: $Vi(mean) = \beta 0 + \beta X + \varepsilon$, where V was the *z* score of the mean of nicotine and placebo conditions on the *i*th voxel. The *t* statistics of β tested the main effect of FTND (*X*). To investigate whether the effect of FTND on cingulate connectivity was secondary to covariates such as long-term smoking exposure, nicotine level, and blood pressure, exploratory regression analyses were performed to examine the relative contribution of addiction severity and each covariate. The β of FTND represented the independent contributions of FTND to the functional connectivity after controlling for the covariate.

NICOTINE EFFECTS ON CINGULATE CONNECTIVITY

To identify nicotine effects on cingulate functional connectivity, paired sample *t* tests were performed on *z*-score maps to assess placebo vs nicotine differences for each ROI.

For clinical data, paired *t* tests were used to examine nicotine vs placebo effect on side effects, withdrawal symptoms, and nicotine and carbon monoxide measures. Pearson correlations were used to examine relationships between clinical and nicotine addiction parameters.

RESULTS

NICOTINE AND DEMOGRAPHIC INFORMATION

Participants were 35.7 (11.1) (mean [SD]) years of age, had 13.0 (1.8) years of education, started smoking at 16.9 (5.7) years of age, and became regular smokers at 18.9 (5.7) years of age. Their nicotine addiction severity, as measured by the FTND, was 4.3 (2.4). Lifetime exposure to cigarette smoking was 15.6 (10.9) pack-years. Changes in withdrawal, side effect symptoms, and mood were not statistically different between placebo and nicotine conditions (**Table 1**). Withdrawal symptoms assessed with time (before and after imaging) and drug (nicotine vs placebo) used as repeated measures also did not show a significant time × drug interaction ($F_{1,18}$=0.42, *P*=.52) or main effect of drug (*P*=.21) or time (*P*=.09). However, change in systolic blood pressure was significantly greater in the nicotine as compared with the placebo condition (*P*=.05). The FTND score significantly correlated with carbon monoxide level before placebo (r=0.53, *P*=.02) or nicotine patch (r=0.61, *P*=.006), but not with nicotine plasma level in placebo (r=0.24, *P*=.35) or nicotine (r=0.29, *P*=.28) conditions, confirming that nicotine level by itself is a state measure and is not directly related to addiction severity.

CINGULATE FUNCTIONAL CONNECTIVITY

The connectivity maps of each cingulate seed ROI ($P_{corrected}$<.05, corresponding to $P_{uncorrected}$<.001 and a cluster size of 810 mm^3) are presented in **Figure 2** (see also the eFigure, http://www.archgenpsychiatry.com). In general, the strongest connectivity of each cingulate ROI was adjacent to its seed region. Nonadjacent regions also showed significant connectivity associated with each cingulate subregion. Specifically, the sACC showed significant blood oxygenation level–dependent synchrony with dACC, medial wall of the superior frontal and orbitofrontal cortex, caudate, middle temporal cortex, precuneus, and vPCC. The oACC showed connectivity with sACC, dACC, superior frontal cortex, middle temporal cortex, insula, caudate, ventral striatum, precentral cortex, and precuneus. The dACC showed connectivity with sACC; oACC; superior frontal, orbitofrontal, and dorsolateral prefrontal cortex; dorsal and ventral striatum; and thalamus. The MCC showed connectivity with dACC, superior and middle frontal cortex, PCC, insula, superior temporal cortex, inferior parietal cortex, thalamus, precuneus/cuneus, and precentral cortex. The dPCC showed connectivity with PCC, precuneus, cuneus,

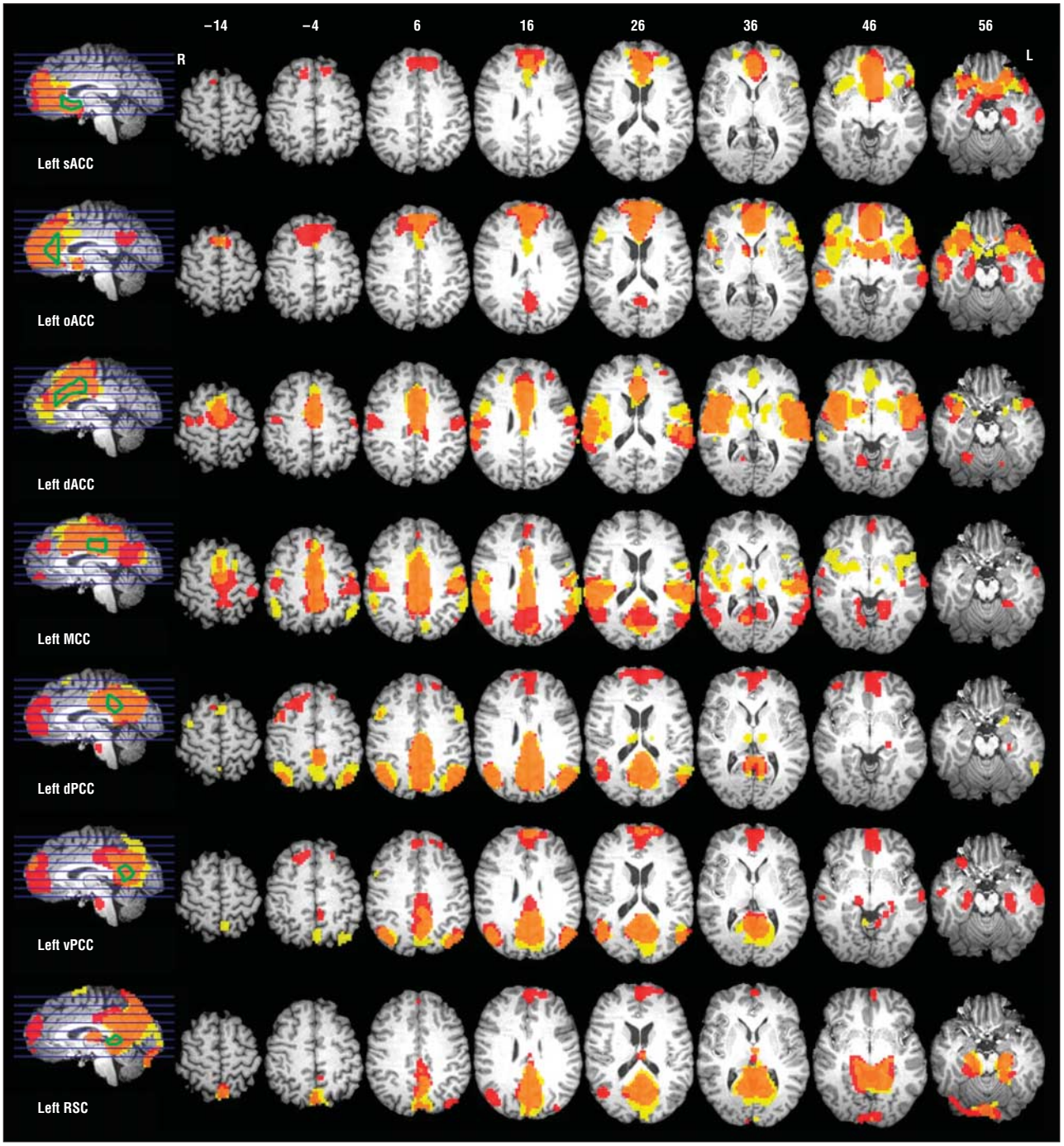

Figure 2. Resting-state functional connectivity maps between each of the left cingulate regions of interest (ROIs) and the rest of the brain ($P_{corrected} < .05$). (See the eFigure for the right cingulate maps.) Maps for nicotine (red) and placebo (yellow) were generated separately and then overlaid together for display purposes; orange indicates overlap. The boundary of the ROIs from 1 subject (green) is overlaid to indicate the approximate locations and sizes of the ROIs in relation to the corresponding functional connectivity maps. Although the connectivity maps from each condition were based on statistically significant connectivity, the overlap or nonoverlap in this display does not imply statistically significant differences between nicotine and placebo conditions. See the legend to Figure 1 for an explanation of the abbreviations.

middle frontal and orbitofrontal gyrus, and thalamus (left side only). The vPCC showed connectivity with PCC, precuneus, cuneus, lingual gyrus, angular gyrus, middle and superior temporal gyrus, inferior parietal gyrus, medial superior and middle frontal gyrus, and parahippocampal gyrus (right side only). The RSC showed connectivity with PCC, postcentral cortex, precuneus, cuneus, parahippocampal/fusiform gyrus, thalamus, superior frontal gyrus (left side only), medial precentral area, left cerebellum, and superior temporal gyrus.

CINGULATE CONNECTIVITY AND NICOTINE ADDICTION SEVERITY

Voxelwise regression analyses showed no significant interaction between FTND score and drug condition in any

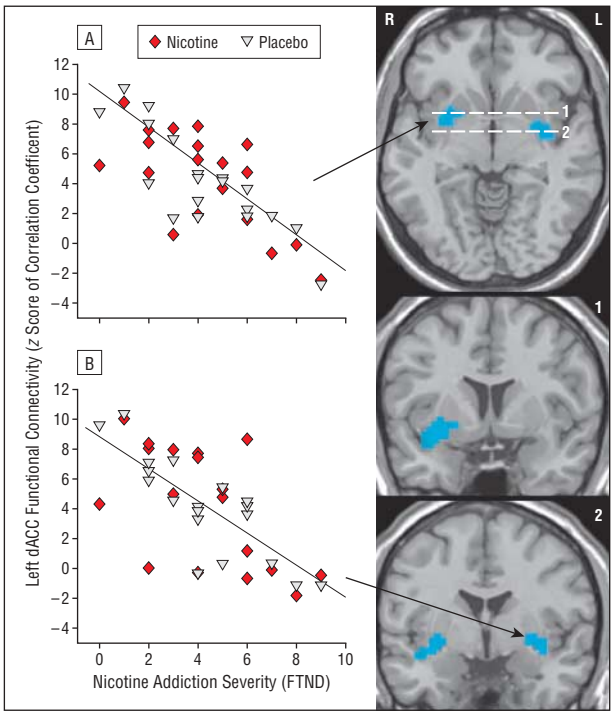

Figure 3. Negative correlations between Fagerström Test for Nicotine Dependence (FTND) and left dorsal anterior cingulate cortex (dACC)–bilateral striatum functional connectivity. Two discrete clusters (blue) had significant main effect of FTND. Scatterplot data were based on mean *z* values of the significant clusters. Fit lines indicate correlations from combined nicotine and placebo trials (no significant interaction): A, $r=-0.76$, $P<.001$; B, $r=-0.69$, $P<.001$. See Table 2 for a description of the corresponding anatomic coordinates, the extent of the significant cluster ($P_{corrected}<.05$), and the correlation coefficients of the nicotine and placebo conditions. Dotted lines on the axial image are the corresponding planes of the coronal images (1 and 2).

cingulate functional circuit. In contrast, voxelwise regression analyses for the main effect of FTND score showed that FTND was significantly ($P_{corrected}<.05$, corresponding to $P_{uncorrected}<.001$ and a cluster size of 243-405 mm^3) and negatively correlated with 3 coactivated circuits: between left dACC and bilateral striatum (**Figure 3**) and between right dACC and right striatum (**Figure 4**). The extent and coordinates of these findings are listed in **Table 2**. Correlation coefficients for each condition were calculated by extracting the mean *z* score of each significant cluster and correlating it with the FTND score. All 3 cingulate-striatal correlations remained significant even after a Bonferroni correction for 14 comparisons ($P<.004$) in the main analysis where nicotine condition and placebo condition were combined (because there was no interaction). However, when we separated nicotine condition and placebo condition as an exploratory analysis, all 3 connectivities remained significant in the placebo condition but only 1 was significant in the nicotine condition. Note that these correlations were present and statistically significant in both the placebo and nicotine conditions, indicating that nicotine did not remove the negative correlations.

To investigate whether the effect of FTND on the dACC-striatal connectivity could be secondary to long-term exposure to smoking, rather than addiction per se, exploratory regression analyses were performed to examine the relative contribution of long-term exposure (pack-years). Analyses were carried out in placebo and nicotine conditions separately for each circuit. The FTND correlations remained significant in all 3 dACC-striatal functional connectivity paths in the placebo (n=19, $\beta=-0.88$ to -0.95, $t=-6.14$ to -7.27, all $P\leq.001$) and nicotine (all $\beta=-0.56$ to -0.70, $t=-2.50$ to -3.56, $P=.02$ to .003) conditions, after controlling for long-term exposure.

Nicotine plasma concentration during imaging also could have influenced the contribution of FTND to the ACC-striatal path. We repeated the preceding analyses with the use of nicotine level as a predictor. The FTND remained negatively correlated with all 3 dACC-striatal functional connectivity scores in both placebo (n=17, all $\beta\leq-0.78$, all $t\leq-4.65$, all $P<.001$) and nicotine (n=16, all $\beta\leq-0.61$, all $t\leq-2.84$, all $P\leq.01$) conditions after controlling for nicotine levels. The FTND also remained significantly correlated with the corresponding dACC-striatal connectivity after controlling for age and sex (data not shown). Taken together, these findings do not support the conclusion that the negative correlations between addiction severity and the dACC-striatal connectivity were substantially biased by long-term smoking exposure, nicotine level during imaging, age, or sex.

Finally, we conducted exploratory regression analyses using the 7 *DSM-IV* criteria for nicotine dependence as predictors. The *DSM-IV* criteria together significantly contributed to the FTND-derived dACC-striatum functional connectivities (R^2 change, 0.58-0.67 for the 3 connectivities; all $P<.001$). Within the models, the functional connectivities were most closely associated with *DSM-IV*–defined tolerance (standardized coefficients $\beta=-0.69$ to -0.79 for the 3 connectivities, all $P<.001$) and, to a lesser extent, withdrawal ($\beta=-0.34$ for the right dACC-striatum connectivity, $P=.02$). These findings are consistent with the symptoms (tolerance and withdrawal) typically contributing to FTND scores in tobacco smokers.

NICOTINE EFFECTS ON CINGULATE CONNECTIVITY

Voxelwise paired *t* tests showed that short-term nicotine administration significantly enhanced the coherence strength of several cingulate functional connectivity paths compared with the placebo condition ($P_{corrected}<.05$). The coordinates having significant nicotine effects are presented in **Table 3**. **Figure 5** illustrates the increased connectivity after nicotine administration between seed ROIs and these locations. The *z* scores of these 7 circuits were significantly different between nicotine and placebo conditions (paired *t* tests, $t=4.1$-5.2, $P\leq.001$) after Bonferroni correction for 14 ROI comparisons (.05/14=.003). A consistent pattern of nicotine effects was seen in the functional connectivity between PCC ROIs and frontal midline structures, including orbitofrontal, medial superior frontal, and anterior cingulate regions (Figure 5B, F, and G). In addition, left subcallosal ACC showed significantly enhanced connectivity with medial frontal cortex (Figure 5D). Another common pattern was the cingulate connectivity with pa-

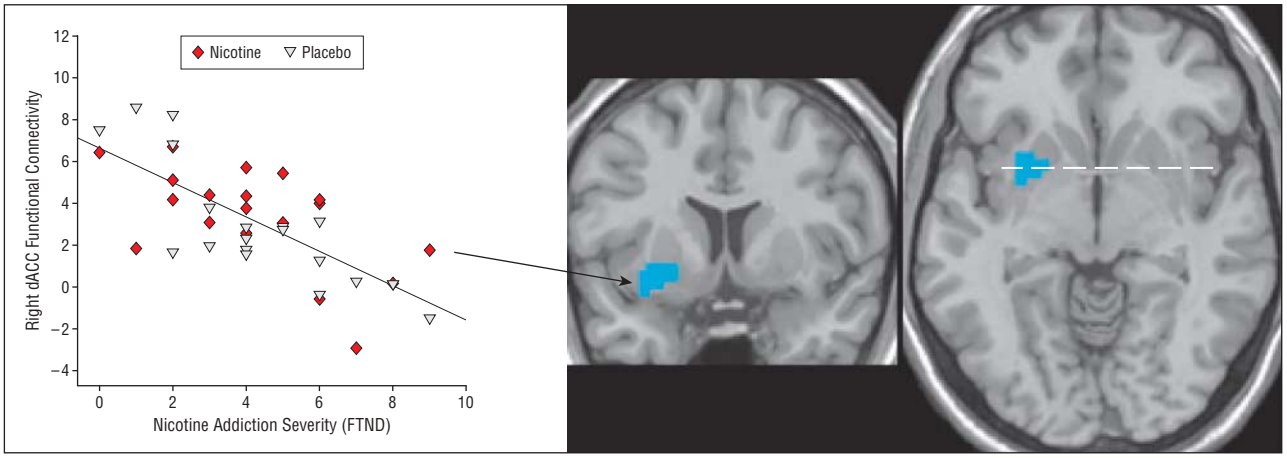

Figure 4. Negative correlation between Fagerström Test for Nicotine Dependence (FTND) and right dorsal anterior cingulate cortex (dACC)–right striatum connectivity. One cluster in the right striatum (blue) had a significant main effect of FTND based on regression analysis (r=−0.72, P<.001). Scatterplot data were based on the mean z value of the significant cluster. See Table 2 for a description of the corresponding anatomic coordinates.

Table 2. Effects of Nicotine Addiction Severity (FTND) on Cingulate Functional Connectivity

Seed ROIs	Co-activating Locations[a]	Volume, mm³	Talairach Coordinates of Maxima			Placebo and Nicotine Trials Combined		Placebo Trials Alone		Nicotine Trials Alone	
			x	y	z	*r* Value	*P* Value	*r* Value	*P* Value	*r* Value	*P* Value
Left dACC	Right striatum	1242	31	−4	−5	−0.76	<.001	−0.84	<.001	−0.68	<.001
	Left striatum	702	−35	−13	−2	−0.69	<.001	−0.83	<.001	−0.57	.01[b]
Right dACC	Right striatum	945	27	−3	−4	−0.72	<.001	−0.82	<.001	−0.60	.007[b]

Abbreviations: dACC, dorsal anterior cingulate cortex; FTND, Fagerström Test for Nicotine Dependence; ROIs, regions of interest.
[a]Right striatum, a more anteroventral cluster than left striatum, included parts of the putamen, ventral striatum, and claustrum. The edge of the cluster also overlapped with the insula, the amygdala, and the parahippocampal gyrus. Left striatum included part of putamen, caudate tail, claustrum, and insula.
[b]Not significant if Bonferroni correction is applied for 14 comparisons

rietal regions, including connectivity between left dACC and superior parietal lobule and the postcentral gyrus, and between the right MCC and the inferior parietal lobule and the postcentral gyrus (Figure 5A and E). Nicotine also enhanced a relatively "local" circuit between the dPCC and vPCC (Figure 5C). Notably, and in contrast, there was no indication that nicotine significantly enhanced any of the 3 ACC-striatal functional connectivity circuits, even with paired t tests. Finally, all nicotine effects were in the positive (enhanced) direction; nicotine never significantly reduced synchronized activity between the cingulate and any other region of the brain.

COMMENT

This study identified non–task-driven, resting-state functional networks associated with discrete cingulate subregions and examined the relationship between an established marker for nicotine addiction and each cingulate circuit. We report what we believe is the novel finding that the severity of nicotine addiction was inversely associated with the strength of the coherent activity between dACC and striatum, ie, the more severe the addiction, the weaker the functional connectivity. Critically, short-term nicotine challenge did not abolish these correlations. In contrast, as part of a double dissociation, short-term nicotine administration did enhance the coherence of other cingulate-cortical circuits that were not correlated with nicotine addiction.

The dACC-striatal functional connectivity paths coincide with known "hard-wired" pathways.[47-49] Baleydier and Mauguiere[47] and others[48,49] noted that the anterior cingulate gyrus (area 24) is connected with the caudate nucleus, the claustrum, and the lateral frontal and the posterior parietal (area 7) cortices. Others also showed that ACC projects to the ventromedial regions of the caudate nucleus and putamen.[50] These fibers are also described as the striatal fibers that are branches from the cingulate bundle,[48,51] all of which provide a putative anatomic basis for the functional connectivity observations.

The FTND is an established clinical and genetic trait marker of nicotine addiction and has a high heritability of around 0.72 to 0.75.[32,33] Its validity in marking nicotine addiction is further supported by association studies using FTND as a primary phenotype, which have identified nicotinic acetylcholine receptor variants contributing to nicotine addiction.[52,53] By showing significant correlations with FTND, we can hypothesize that resting-state synchronized activity in the dACC-striatum circuits may serve as a circuitry-level endophenotypic marker for nicotine addiction. Anatomically, the identified striatal clusters mainly include the putamen and its transi-

Table 3. Cingulate Functional Connectivity Circuits Enhanced by Nicotine

	Functionally Connected Regions Enhanced by Nicotine						
					Talairach Coordinates of Maxima		
Seed ROIs	Location	Laterality	Brodmann Area	Volume, mm^3	x	y	z
Left dACC	Superior parietal lobule and postcentral gyrus	Contralateral	5/7	999	19	−44	62
Left vPCC	Medial frontal gyrus and ACC	Bilateral	10/32	1296	0	46	12
Left dPCC	Posterior cingulate	Bilateral	23/30	648	−1	−54	19
Left sACC	Medial frontal gyrus	Ipsilateral	8	459	−11	38	44
Right MCC	Postcentral gyrus and inferior parietal lobule	Contralateral	5/40	1107	−30	−37	56
Right vPCC	Medial frontal gyrus	Bilateral	9/10	378	−1	47	13
Right dPCC	Medial frontal gyrus and ACC	Bilateral	9/10	459	3	59	19

Abbreviations: ACC, anterior cingulate cortex; dACC, dorsal ACC; dPCC, dorsal posterior cingulate cortex; MCC, middle cingulate cortex; ROIs, regions of interest; sACC, subcallosal ACC; vPCC; ventral posterior cingulate cortex.

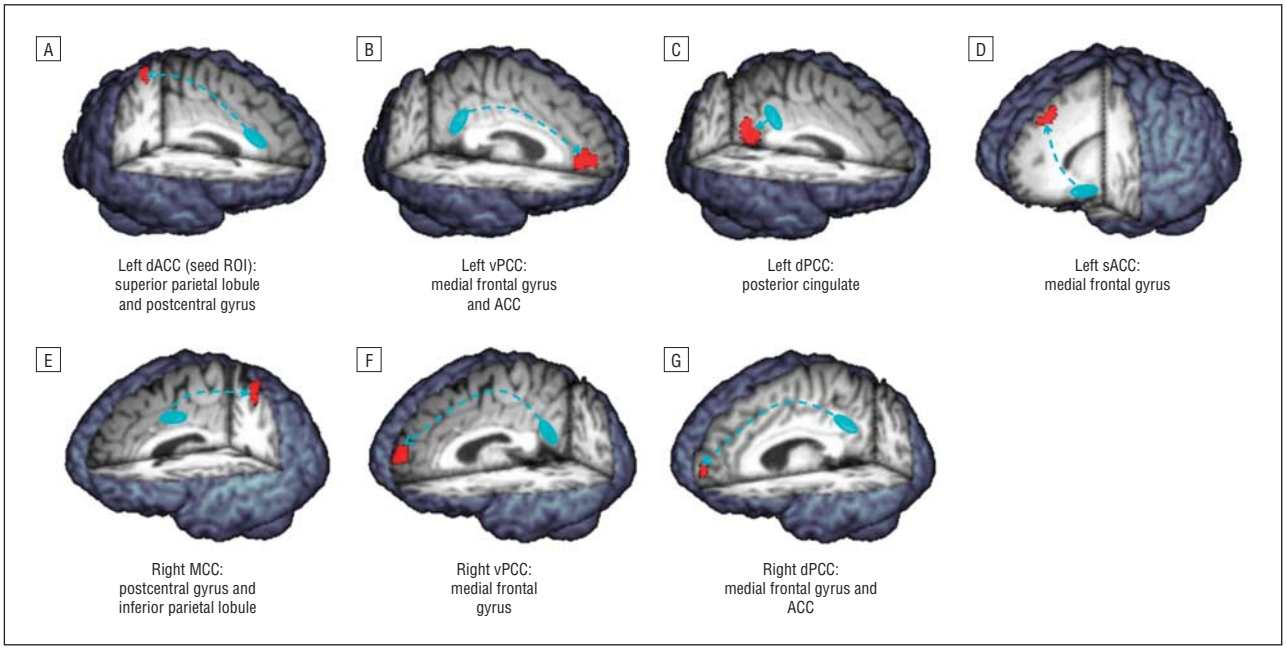

Figure 5. Significant main effect of drug on cingulate circuitry based on paired *t* test results. Seven (A-G) resting-state functional connectivity pathways were statistically enhanced by nicotine administration (red) when compared with placebo. See Table 3 for abbreviations, coordinates, and the extent of each significant cluster. There was never a statistically significant reduction in functional connectivity by nicotine. Ovals indicate the seed ROIs. Arrows infer the relationship between the seed ROI and the areas that were affected by nicotine and do not imply directionality of the functional connectivity path. These figures represent the nicotine-placebo differences in Figure 2 that were statistically significant.

tion to the nucleus accumbens, encompassing roughly a transitional zone between dorsal and ventral striatum. The progression of addiction is thought to be associated with initial medial frontal/anterior cingulate cortex executive control over ventral striatal reinforcement mechanisms, which, as the addictive processes continue, are replaced by more habit-driven, dorsal striatal activity.[54,55] The finding that more severe nicotine addiction is associated with weaker functional connectivity between ACC and striatum may be tied to an underlying dysfunction associated with addictive behaviors that are modulated by this circuit.

We observed that nicotine, even at high plasma levels (34.3 [13.1] ng/mL [to convert nicotine to micromoles per liter, multiply by 0.006164]), did not substantially alter the negative correlations between FTND score and the ACC-striatal coherence. Although there were nonsignificant numerical reductions in the strength of the negative correlations during nicotine administration in the post hoc exploratory analyses, the significant negative correlations were not abolished. In other words, nicotine administration alone, at least for the short duration used in this study, did not robustly influence the circuit level abnormalities associated with nicotine addiction severity. In contrast, nicotine did significantly enhance the functional connectivity of several cingulate-cortical networks, which also seem to follow the presence of known fiber tracks interconnecting these regions. For example, one such connectivity path is between PCCs and the orbitofrontal cortex/ACC. Anatomically, PCC is linked with

the medial orbitoprefrontal cortex, the medial extension of the prefrontal cortex, and the ACC by the cingulate bundle.[25,47,49,51] Another example, the ACC/MCC–parietal lobe network, is a circuit with known reciprocal fiber connections.[49,51] Notably, all of the observed nicotine effects were to enhance the higher-order, isocortical functional connections. Whether this corticocortical enhancement of functional connectivity is channeled directly via these structures cannot be determined with the present technology, although this may be suggested by the well-established corticocortical fibers linking these regions. That resting-state connectivity strength has been shown to be related to performance on a working memory task also suggests the physiological relevance of our observations.[56]

The apparent contrast between the effects of short-term nicotine on cingulate-neocortical but not cingulate-striatal functional connectivity may be clinically relevant. Although many available treatments have helped to reduce the prevalence of smoking, the efficacy of nicotine replacement therapy has been generally unsatisfactory; for example, nicotine patch treatment yields only about a 10% to 15% long-term quit rate.[57] However, nicotine, even in a single dose, can induce robust, transient enhancement of diverse neurophysiological and cognitive functions (see the introductory material). The mechanisms responsible for this dichotomy are unknown.

On the basis of the current data, we hypothesize that nicotine may improve behavioral tasks through a transient enhancement of distributed cingulate-neocortical or other corticocortical functional networks, regardless of task demands. The observed nicotine-related behavioral and imaging signals in a given experiment may represent the circuits taxed by the specific behavioral task performed and may be reflected by the enhanced cingulate-neocortical connectivity strengths reported herein. Depending on the behavioral tasks during imaging, cingulate activity was shown to have increased[3,12,13,16] or decreased[2,14,58] after nicotine administration. The present resting-state connectivity data offer a new perspective toward resolving these inconsistencies by suggesting that the cingulate involvement in nicotine actions may not be simply local increases or decreases of activity within the cingulate proper, but may be related to enhancement in synchronized activity between cingulate and its functionally connected cortical regions. On the other hand, the FTND correlation data suggest that nicotine addiction is not primarily associated with the coherent activity of the neocortical connections, but rather is associated with a more specific alteration in dACC-striatal connectivity. Short-term administration of nicotine itself does not substantially affect the strength of this connectivity circuit, which may in part help explain the low rate of smoking cessation with nicotine replacement therapy. Our findings offer potential brain circuitry–level mechanisms to explain the incongruent data of clear nicotine effects on cognitive enhancement vs its limited effect on treating nicotine addiction.

Task-independent, functionally coherent resting-state networks are thought to represent intrinsically synchronized activity of the brain and have been termed the *default-mode network*.[11,17] The most consistent regions associated with this network are PCC, ACC, and medial frontal regions,[10,11] along with several frequently detected areas such as superior and inferior parietal lobule and precuneus.[10,11,17,59] The default-mode network is reliably detected regardless of whether a person keeps his or her eyes closed or open during the resting state.[11,17] The default-mode maps identified from the PCC and ACC subregions in this study were remarkably similar to findings of the corresponding cingulate seed ROIs from previous studies.[11,60] As illustrated by our data, the potential functional role of the default-mode connectivity is intriguing. The default-state connectivity was initially proposed to represent a "sentinel" role of the resting but awake brain to broadly evaluate information from external and internal milieu.[10] Our data show that this resting-state network is also subject to pharmacological manipulations.

The steady-state nicotine effect on neocortical connectivity after patch administration does not necessarily imply a similar effect during more rapid nicotine delivery as provided by cigarette smoking. The current patch design identifies the pharmacologic action of nicotine on brain circuit dynamics. Replication studies using faster nicotine delivery systems, such as nasal spray or smoking itself, are warranted.

Although we did find mildly elevated systolic pressure in the nicotine condition, it is likely that our findings were due to nicotine-induced neuronal activity rather than secondary to nonspecific cardiovascular changes. Blood pressure changes do not correlate with cortical brain activation.[61] A recent report demonstrated no effect of nicotine on finger tapping–induced blood oxygenation level–dependent activation.[62] The correlations seen between FTND and regional connectivity were similar between the nicotine and placebo conditions, which also argues against a nonspecific vascular effect.

In conclusion, this study demonstrated that nicotine increases cingulate-neocortical functional connectivity coherence strength during the resting state. However, this short-term nicotine challenge does not significantly alter the cingulate-striatal circuitry that was associated with the severity of nicotine addiction, suggesting that nicotine replacement does not necessarily correct the network abnormalities associated with nicotine addiction. The abnormal resting-state cingulate-striatal functional connectivity may serve as an in vivo biomarker for testing new, potentially more effective, nicotine addiction therapeutics. Our study further suggests that the non–task-dependent resting-state imaging approach might also be useful to characterize pharmacologically induced changes associated with nicotine and perhaps other pharmacological-imaging studies.

Submitted for Publication: April 18, 2008; final revision received July 30, 2008; accepted August 13, 2008.
Correspondence: L. Elliot Hong, MD, Maryland Psychiatric Research Center, Department of Psychiatry, University of Maryland School of Medicine, PO Box 21247, Baltimore, MD 21228 (ehong@mprc.umaryland.edu).
Author Contributions: Drs Hong, Gu, and Yang contributed equally to this work.
Financial Disclosure: None reported.

Funding/Support: This study was supported by National Institutes of Health grants MH70644, 79172, 49826, 77852, 68580, and N01-DA-5-9909; the National Institute on Drug Abuse Intramural Research Program; Neurophysiology Core of the University of Maryland General Clinical Research Center (M01-RR16500); and the Maryland Cigarette Restitution Fund Program–Other Tobacco-Related Diseases Research Grant.

Additional Information: The eFigure is available at http://www.archgenpsychiatry.com.

REFERENCES

1. Levin ED, Rezvani AH. Development of nicotinic drug therapy for cognitive disorders. *Eur J Pharmacol*. 2000;393(1-3):141-146.
2. Hahn B, Ross TJ, Yang Y, Kim I, Huestis MA, Stein EA. Nicotine enhances visuospatial attention by deactivating areas of the resting brain default network. *J Neurosci*. 2007;27(13):3477-3489.
3. Lawrence NS, Ross TJ, Stein EA. Cognitive mechanisms of nicotine on visual attention. *Neuron*. 2002;36(3):539-548.
4. Myers CS, Taylor RC, Moolchan ET, Heishman SJ. Dose-related enhancement of mood and cognition in smokers administered nicotine nasal spray. *Neuropsychopharmacology*. 2008;33(3):588-598.
5. Kumari V, Gray JA. Smoking withdrawal, nicotine dependence and prepulse inhibition of the acoustic startle reflex. *Psychopharmacology (Berl)*. 1999;141(1):11-15.
6. Mancuso G, Andres P, Ansseau M, Tirelli E. Effects of nicotine administered via a transdermal delivery system on vigilance: a repeated measure study. *Psychopharmacology (Berl)*. 1999;142(1):18-23.
7. McClernon FJ, Gilbert DG, Radtke R. Effects of transdermal nicotine on lateralized identification and memory interference. *Hum Psychopharmacol*. 2003;18(5):339-343.
8. Swanson LW, Simmons DM, Whiting PJ, Lindstrom J. Immunohistochemical localization of neuronal nicotinic receptors in the rodent central nervous system. *J Neurosci*. 1987;7(10):3334-3342.
9. Nybäck H, Nordberg A, Langstrom B, Halldin C, Hartvig P, Ahlin A, Swahn CG, Sedvall G. Attempts to visualize nicotinic receptors in the brain of monkey and man by positron emission tomography. *Prog Brain Res*. 1989;79:313-319.
10. Raichle ME, MacLeod AM, Snyder AZ, Powers WJ, Gusnard DA, Shulman GL. A default mode of brain function. *Proc Natl Acad Sci U S A*. 2001;98(2):676-682.
11. Greicius MD, Krasnow B, Reiss AL, Menon V. Functional connectivity in the resting brain: a network analysis of the default mode hypothesis. *Proc Natl Acad Sci U S A*. 2003;100(1):253-258.
12. Grünwald F, Schrock H, Kuschinsky W. The effect of an acute nicotine infusion on the local cerebral glucose utilization of the awake rat. *Brain Res*. 1987;400(2):232-238.
13. Stein EA, Pankiewicz J, Harsch HH, Cho JK, Fuller SA, Hoffmann RG, Hawkins M, Rao SM, Bandettini PA, Bloom AS. Nicotine-induced limbic cortical activation in the human brain: a functional MRI study. *Am J Psychiatry*. 1998;155(8):1009-1015.
14. Ernst M, Matochik JA, Heishman SJ, Van Horn JD, Jons PH, Henningfield JE, London ED. Effect of nicotine on brain activation during performance of a working memory task. *Proc Natl Acad Sci U S A*. 2001;98(8):4728-4733.
15. Giessing C, Fink GR, Rosler F, Thiel CM. fMRI data predict individual differences of behavioral effects of nicotine: a partial least square analysis. *J Cogn Neurosci*. 2007;19(4):658-670.
16. Kumari V, Gray JA, ffytche DH, Mitterschiffthaler MT, Das M, Zachariah E, Vythelingum GN, Williams SC, Simmons A, Sharma T. Cognitive effects of nicotine in humans: an fMRI study. *Neuroimage*. 2003;19(3):1002-1013.
17. Fransson P. Spontaneous low-frequency BOLD signal fluctuations: an fMRI investigation of the resting-state default mode of brain function hypothesis. *Hum Brain Mapp*. 2005;26(1):15-29.
18. Shulman GL, Fiez JA, Corbetta M, Buckner RL, Miezin FM, Raichle ME, Petersen SE. Common blood flow changes across visual tasks, II: decreases in cerebral cortex. *J Cogn Neurosci*. 1997;9:648-663.
19. Gusnard DA, Raichle ME, Raichle ME. Searching for a baseline: functional imaging and the resting human brain. *Nat Rev Neurosci*. 2001;2(10):685-694.
20. Smith AT, Williams AL, Singh KD. Negative BOLD in the visual cortex: evidence against blood stealing. *Hum Brain Mapp*. 2004;21(4):213-220.
21. Shmuel A, Augath M, Oeltermann A, Logothetis NK. Negative functional MRI response correlates with decreases in neuronal activity in monkey visual area V1. *Nat Neurosci*. 2006;9(4):569-577.
22. Vincent JL, Patel GH, Fox MD, Snyder AZ, Baker JT, Van Essen DC, Zempel JM, Snyder LH, Corbetta M, Raichle ME. Intrinsic functional architecture in the anaesthetized monkey brain. *Nature*. 2007;447(7140):83-86.
23. Johnston JM, Vaishnavi SN, Smyth MD, Zhang D, He BJ, Zempel JM, Shimony JS, Snyder AZ, Raichle ME. Loss of resting interhemispheric functional connectivity after complete section of the corpus callosum. *J Neurosci*. 2008;28(25):6453-6458.
24. Morris R, Paxinos G, Petrides M. Architectonic analysis of the human retrosplenial cortex. *J Comp Neurol*. 2000;421(1):14-28.
25. Vogt BA, Vogt LJ, Perl DP, Hof PR. Cytology of human caudomedial cingulate, retrosplenial, and caudal parahippocampal cortices. *J Comp Neurol*. 2001;438(3):353-376.
26. Vogt BA, Vogt L. Cytology of human dorsal midcingulate and supplementary motor cortices. *J Chem Neuroanat*. 2003;26(4):301-309.
27. Vogt BA, Vogt L, Laureys S. Cytology and functionally correlated circuits of human posterior cingulate areas. *Neuroimage*. 2006;29(2):452-466.
28. Fornito A, Whittle S, Wood SJ, Velakoulis D, Pantelis C, Yucel M. The influence of sulcal variability on morphometry of the human anterior cingulate and paracingulate cortex. *Neuroimage*. 2006;33(3):843-854.
29. McCormick LM, Ziebell S, Nopoulos P, Cassell M, Andreasen NC, Brumm M. Anterior cingulate cortex: an MRI-based parcellation method. *Neuroimage*. 2006;32(3):1167-1175.
30. First MB, Spitzer RL, Gibbon M, Williams JBW. *Structured Clinical Interview for* DSM-IV *Axis I Disorders*. Arlington, VA: American Psychiatric Publishing Inc; 1997.
31. Heatherton TF, Kozlowski LT, Frecker RC, Fagerstrom KO. The Fagerstrom Test for Nicotine Dependence: a revision of the Fagerstrom Tolerance Questionnaire. *Br J Addict*. 1991;86(9):1119-1127.
32. Kendler KS, Neale MC, Sullivan P, Corey LA, Gardner CO, Prescott CA. A population-based twin study in women of smoking initiation and nicotine dependence. *Psychol Med*. 1999;29(2):299-308.
33. Vink JM, Willemsen G, Boomsma DI. Heritability of smoking initiation and nicotine dependence. *Behav Genet*. 2005;35(4):397-406.
34. Hughes JR, Higgins ST, Bickel WK. Nicotine withdrawal versus other drug withdrawal syndromes: similarities and dissimilarities. *Addiction*. 1994;89(11):1461-1470.
35. Parrott AC, Garnham NJ, Wesnes K, Pincock C. Cigarette smoking and abstinence: comparative effects upon cognitive task performance and mood state over 24 hours. *Hum Psychopharmacol*. 1996;11(5):391-400.
36. Cox RW. Software for analysis and visualization of functional magnetic resonance neuroimages. *Comput Biomed Res*. 1996;29(3):162-173.
37. Oakes TR, Johnstone T, Ores Walsh KS, Greischar LL, Alexander AL, Fox AS, Davidson RJ. Comparison of fMRI motion correction software tools. *Neuroimage*. 2005;28(3):529-543.
38. Biswal B, Yetkin FZ, Haughton VM, Hyde JS. Functional connectivity in the motor cortex of resting human brain using echo-planar MRI. *Magn Reson Med*. 1995;34(4):537-541.
39. Lowe MJ, Mock BJ, Sorenson JA. Functional connectivity in single and multislice echoplanar imaging using resting-state fluctuations. *Neuroimage*. 1998;7(2):119-132.
40. Cordes D, Haughton VM, Arfanakis K, Carew JD, Turski PA, Moritz CH, Quigley MA, Meyerand ME. Frequencies contributing to functional connectivity in the cerebral cortex in "resting-state" data. *AJNR Am J Neuroradiol*. 2001;22(7):1326-1333.
41. Fox MD, Snyder AZ, Vincent JL, Corbetta M, Van Essen DC, Raichle ME. The human brain is intrinsically organized into dynamic, anticorrelated functional networks. *Proc Natl Acad Sci U S A*. 2005;102(27):9673-9678.
42. Lund TE, Madsen KH, Sidaros K, Luo WL, Nichols TE. Non-white noise in fMRI: does modelling have an impact? *Neuroimage*. 2006;29(1):54-66.
43. Ashburner J, Friston KJ. Unified segmentation. *Neuroimage*. 2005;26(3):839-851.
44. Turken AU, Swick D. Response selection in the human anterior cingulate cortex. *Nat Neurosci*. 1999;2(10):920-924.
45. Ward BD. Simultaneous inference for FMRI data. 2000. http://afni.nimh.nih.gov/afni/doc/manual/AlphaSim. Accessed December 23, 2008.
46. Thirion B, Pinel P, Meriaux S, Roche A, Dehaene S, Poline JB. Analysis of a large fMRI cohort: statistical and methodological issues for group analyses. *Neuroimage*. 2007;35(1):105-120.
47. Baleydier C, Mauguiere F. The duality of the cingulate gyrus in monkey: neuroanatomical study and functional hypothesis. *Brain*. 1980;103(3):525-554.
48. Schmahmann JD, Pandya DN. *Fiber Pathways of the Brain*. New York, NY: Oxford University Press; 2006.
49. Vogt BA, Pandya DN. Cingulate cortex of the rhesus monkey, II: cortical afferents. *J Comp Neurol*. 1987;262(2):271-289.
50. Selemon LD, Goldman-Rakic PS. Longitudinal topography and interdigitation of corticostriatal projections in the rhesus monkey. *J Neurosci*. 1985;5(3):776-794.

51. Mufson EJ, Pandya DN. Some observations on the course and composition of the cingulum bundle in the rhesus monkey. *J Comp Neurol.* 1984;225(1): 31-43.
52. Saccone SF, Hinrichs AL, Saccone NL, Chase GA, Konvicka K, Madden PA, Breslau N, Johnson EO, Hatsukami D, Pomerleau O, Swan GE, Goate AM, Rutter J, Bertelsen S, Fox L, Fugman D, Martin NG, Montgomery GW, Wang JC, Ballinger DG, Rice JP, Bierut LJ. Cholinergic nicotinic receptor genes implicated in a nicotine dependence association study targeting 348 candidate genes with 3713 SNPs. *Hum Mol Genet.* 2007;16(1):36-49.
53. Thorgeirsson TE, Geller F, Sulem P, Rafnar T, Wiste A, Magnusson KP, Manolescu A, Thorleifsson G, Stefansson H, Ingason A, Stacey SN, Bergthorsson JT, Thorlacius S, Gudmundsson J, Jonsson T, Jakobsdottir M, Saemundsdottir J, Olafsdottir O, Gudmundsson LJ, Bjornsdottir G, Kristjansson K, Skuladottir H, Isaksson HJ, Gudbjartsson T, Jones GT, Mueller T, Gottsater A, Flex A, Aben KK, de Vegt F, Mulders PF, Isla D, Vidal MJ, Asin L, Saez B, Murillo L, Blondal T, Kolbeinsson H, Stefansson JG, Hansdottir I, Runarsdottir V, Pola R, Lindblad B, van Rij AM, Dieplinger B, Haltmayer M, Mayordomo JI, Kiemeney LA, Matthiasson SE, Oskarsson H, Tyrfingsson T, Gudbjartsson DF, Gulcher JR, Jonsson S, Thorsteinsdottir U, Kong A, Stefansson K. A variant associated with nicotine dependence, lung cancer and peripheral arterial disease. *Nature.* 2008;452(7187): 638-642.
54. Everitt BJ, Robbins TW. Neural systems of reinforcement for drug addiction: from actions to habits to compulsion. *Nat Neurosci.* 2005;8(11):1481-1489.
55. Kalivas PW, O'Brien C. Drug addiction as a pathology of staged neuroplasticity. *Neuropsychopharmacology.* 2008;33(1):166-180.
56. Hampson M, Driesen NR, Skudlarski P, Gore JC, Constable RT. Brain connectivity related to working memory performance. *J Neurosci.* 2006;26(51):13338-13343.
57. Hyland A, Rezaishiraz H, Giovino G, Bauer JE, Michael CK. Over-the-counter availability of nicotine replacement therapy and smoking cessation. *Nicotine Tob Res.* 2005;7(4):547-555.
58. Stapleton JM, Gilson SF, Wong DF, Villemagne VL, Dannals RF, Grayson RF, Henningfield JE, London ED. Intravenous nicotine reduces cerebral glucose metabolism: a preliminary study. *Neuropsychopharmacology.* 2003;28(4):765-772.
59. Shulman GL, Corbetta M, Buckner RL, Raichle ME, Fiez JA, Miezin FM, Petersen SE. Top-down modulation of early sensory cortex. *Cereb Cortex.* 1997;7(3): 193-206.
60. Margulies DS, Kelly AM, Uddin LQ, Biswal BB, Castellanos FX, Milham MP. Mapping the functional connectivity of anterior cingulate cortex. *Neuroimage.* 2007;37(2):579-588.
61. Grünwald F, Schrock H, Kuschinsky W. The influence of nicotine on local cerebral blood flow in rats. *Neurosci Lett.* 1991;124(1):108-110.
62. Murphy K, Dixon V, LaGrave K, Kaufman J, Risinger R, Bloom A, Garavan H. A validation of event-related fMRI comparisons between users of cocaine, nicotine, or cannabis and control subjects. *Am J Psychiatry.* 2006;163(7):1245-1251.